Thon et al., http://www.jcb.org/cgi/content/full/jcb.201111136/DC1

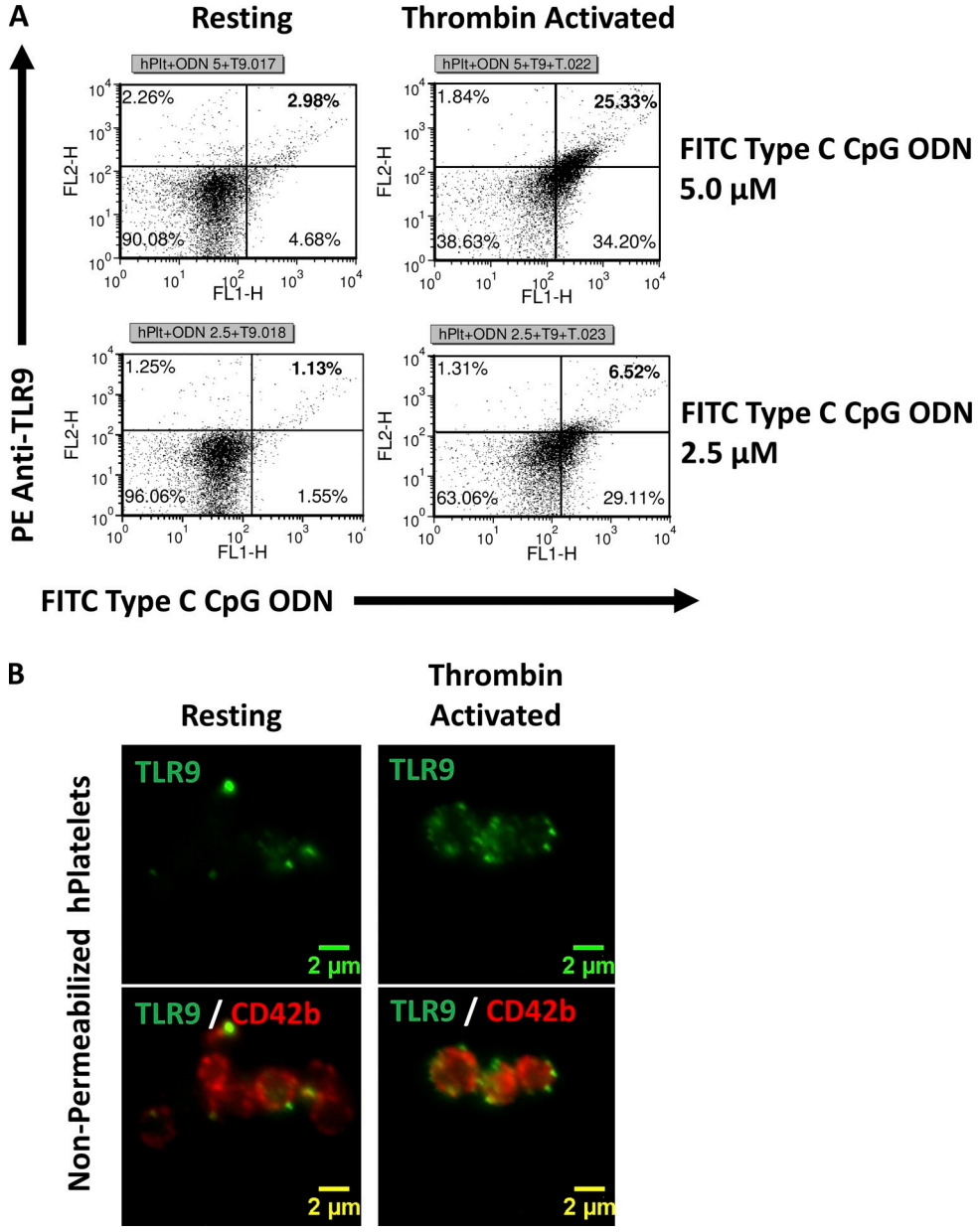

Figure S1. **Surface expression of TLR9 and binding to type C CpG in resting and thrombin-activated human PLTs.** Washed PLTs were collected from human whole blood and examined under resting conditions or after activation with 1 mU/µl thrombin. (A) Flow cytometry was used to measure surface expression of TLR9 and FITC-conjugated type C CpG binding at 5.0- and 2.5-µM concentrations. TLR9 surface expression was significantly increased on PLT activation with thrombin and corresponded with greater levels of FITC-conjugated type C CpG binding on the PLT surface. This association responded in a dose-dependent manner. Percentages of total objects quantified in each quadrant are included in their respective boxes. (B) Wide-field immunofluorescence microscopy was used to visualize surface expression of TLR9 in nonpermeabilized resting and thrombin-activated human PLTs. CD42b is conserved on the resting PLT surface and was used as a marker for the plasma membrane localization of TLR9. Although TLR9 was hardly visible in resting human PLTs, this signal became significantly brighter and more diffuse on thrombin activation, suggesting increased surface expression of the receptor.

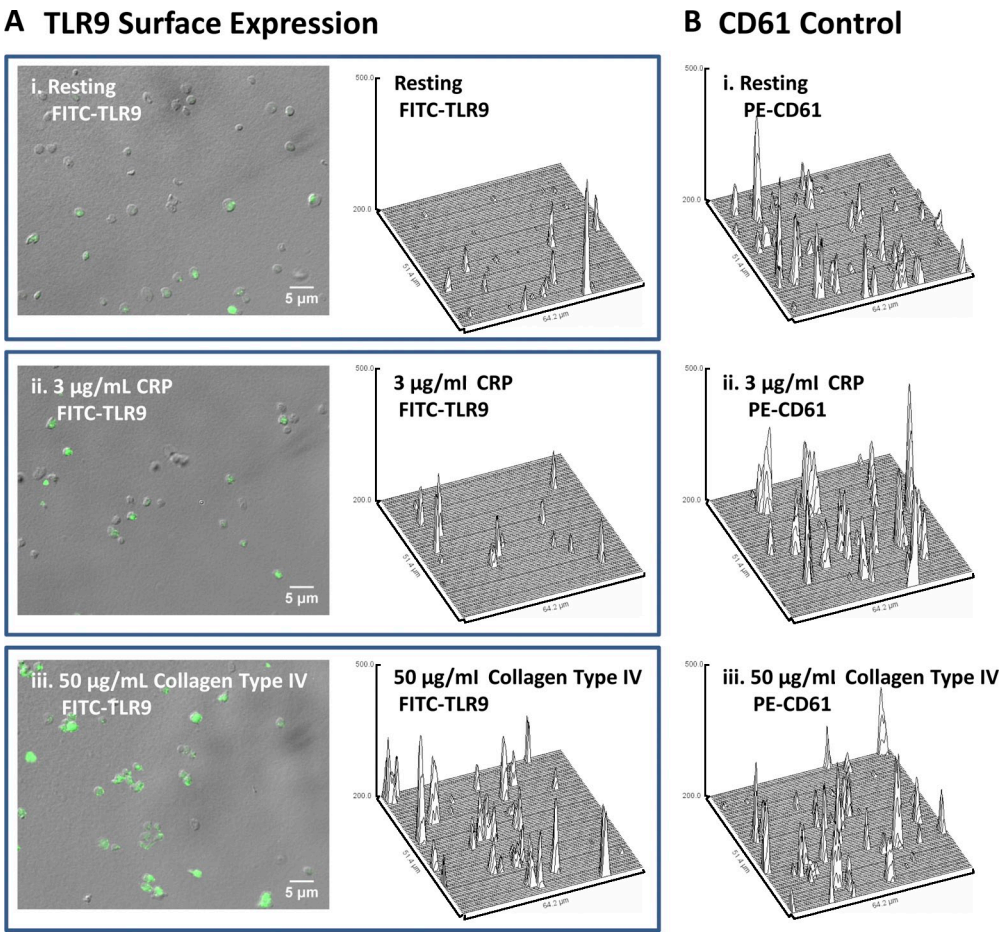

Figure S2. **Increased surface expression of TLR9 in human whole-blood PLTs is not associated with increased surface expression of CD61.** Washed PLTs were collected from human whole blood and examined under resting conditions or after activation with either 3 µg/ml CRP or 50 µg/ml type IV collagen. PLTs were then spun down onto poly-L-lysine–coated glass cover slides and probed for TLR9 or CD61. Wide-field immunofluorescence microscopy was used to visualize surface expression of labeled receptor in nonpermeabilized cells. Images were corrected for background fluorescence, and dynamic range was linearly adjusted equally across all images to display the minimum and maximum intensity pixels. (A) Representative images demonstrating that background levels of TLR9 surface expression detected by flow cytometry are most likely caused by a subpopulation of resting PLTs that express TLR9 at near active levels. Although PLT activation with CRP did not result in a significant increase in the mean fluorescence intensity per field or number of PLTs expressing TLR9 on their surface relative to resting controls, both were drastically elevated in PLTs that had been incubated with type IV collagen. (B) PLT activation with CRP resulted in a significant increase in the mean fluorescence intensity of CD61 expressing PLTs, whereas PLTs that had been incubated with type IV collagen showed no considerable change in mean fluorescence intensity relative to resting controls. These results agree with flow cytometry data (Fig. 1) and suggest that TLR9 and CD61 may localize to distinct granule populations.

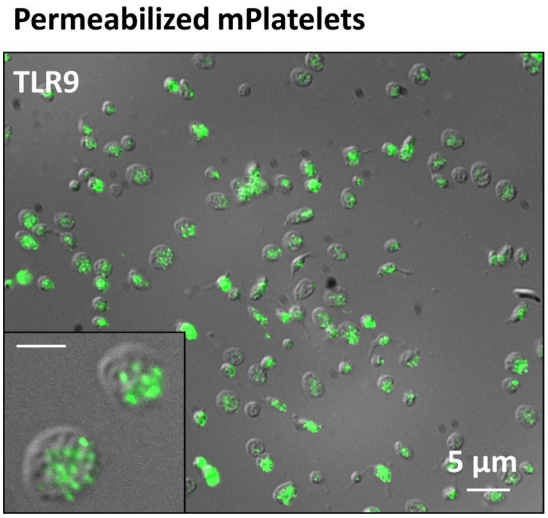

Figure S3. **Murine PLTs express TLR9 in distinct granules along the periphery of the cell, adjacent to the plasma membrane.** Washed murine whole-blood PLTs were spun down onto poly-L-lysine–coated glass coverlids, permeabilized with 0.5% Triton X-100 for 5 min, and probed for TLR9. Samples were examined by wide-field fluorescence microscopy and revealed peripheral labeling of TLR9 in distinct, punctate granules that localized along the cell periphery, adjacent the plasma membrane (as in human PLTs). The inset represents a magnified region outlined by the yellow box in this image. Bar, 2 µm.

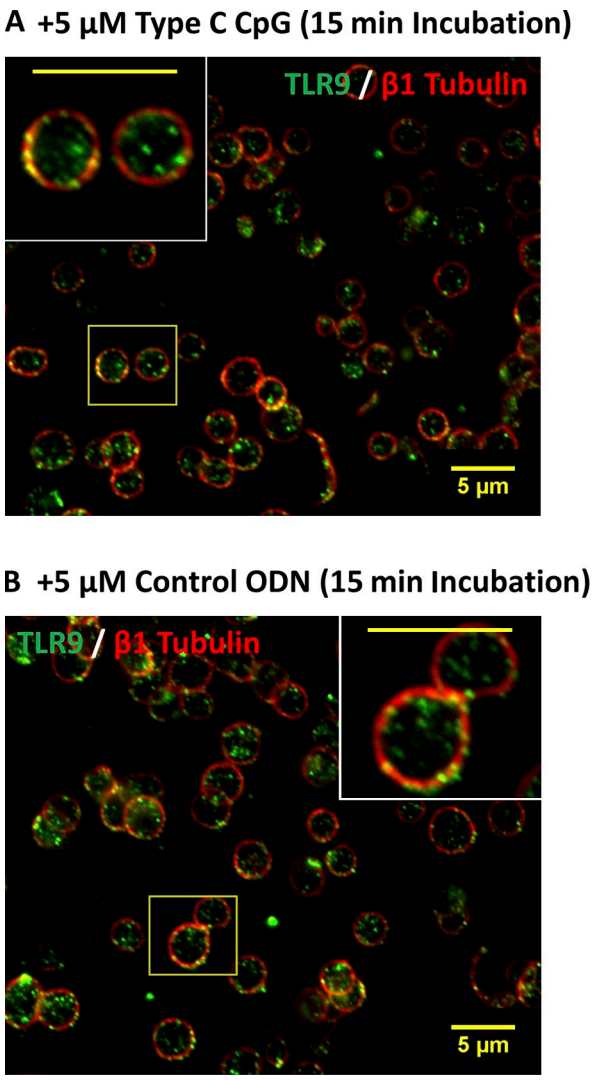

Figure S4. **Incubation of resting human PLTs with type C CpG does not affect overall PLT morphology or TLR9 localization and expression.** (A and B) Washed resting human whole-blood PLTs were first incubated with 5 µM of either type C CpG (A) or a control ODN (B) and then spun down onto poly-L-lysine–coated glass coverlids, permeabilized with 0.5% Triton X-100 for 5 min, and probed for TLR9 and β1-tubulin. Samples were examined by wide-field fluorescence microscopy. Incubation of resting human PLTs with type C CpG did not affect overall PLT morphology or TLR9 localization and expression relative to ODN control. Insets represent magnified regions outlined by the yellow boxes for each image. Bars, 5 µm.

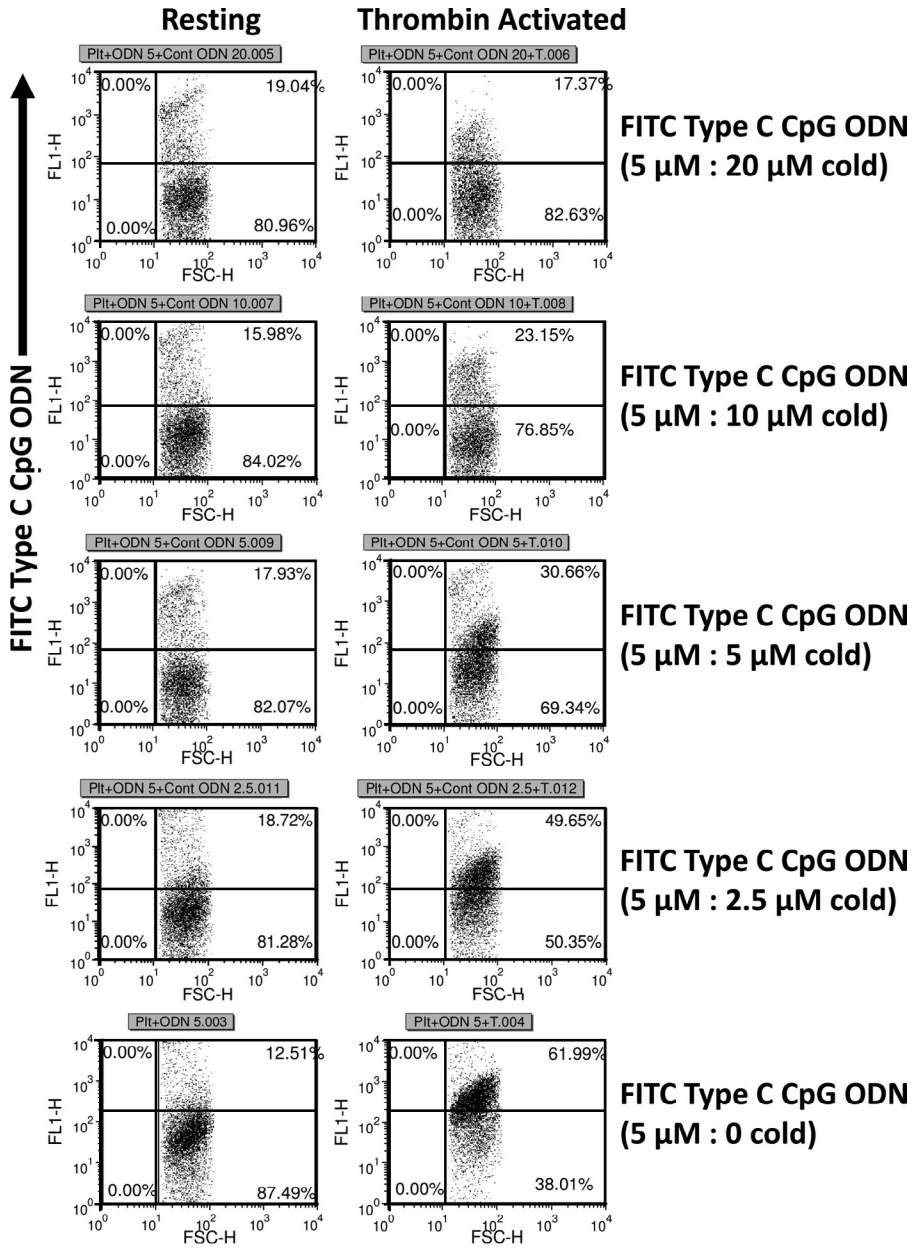

Figure S5. **FITC-conjugated type C CpG behaves like nonconjugated type C CpG with regard to TLR9 binding.** Washed PLTs were collected from human whole blood and examined under resting conditions or after activation with 1 mU/µl thrombin. PLTs were incubated with 5 µM FITC-conjugated type C CpG and decreasing concentrations of unlabeled (cold) type C CpG. Flow cytometry was used to measure FITC-conjugated type C CpG binding to the PLT surface. Thrombin-activated PLTs showed stoichiometrically increased fluorescence that was proportionate with decreasing concentrations of unlabeled type C CpG. Resting human PLTs showed fluorescence profiles that were comparable with the 20 µM of unlabeled type C CpG control at all the concentrations tested. Percentages of total objects quantified in each quadrant are included in their respective boxes. FSC-H, forward scatter height.

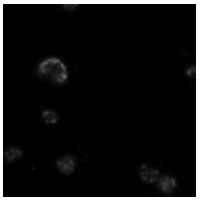

Video 1. **TLR9 colocalizes with PDI in distinct punctuate granules in resting human PLTs probed for TLR9.** Washed human whole-blood PLTs were spun down onto poly-L-lysine–coated glass cover slides, permeabilized with 0.5% Triton X-100 for 5 min, and probed for TLR9. Representative 0.244 µm–step z series were generated by confocal fluorescence microscopy and revealed colocalization of TLR9 and PDI in distinct, punctate granules. Cells were viewed on a microscope (TCS SP2) with a Plan-Apochromat 63×, NA 1.4 oil immersion objective and an optical zoom of 2×. Images were obtained using a CCD camera (ORCA-ER).

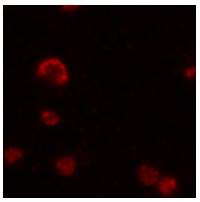

Video 2. **TLR9 colocalizes with PDI in distinct punctuate granules in resting human PLTs probed for PDI.** Washed human whole-blood PLTs were spun down onto poly-L-lysine–coated glass cover slides, permeabilized with 0.5% Triton X-100 for 5 min, and probed for PDI. Representative 0.244 µm–step z series were generated by confocal fluorescence microscopy and revealed colocalization of TLR9 and PDI in distinct, punctate granules. Cells were viewed on a microscope (TCS SP2) with a Plan-Apochromat 63×, NA 1.4 oil immersion objective and an optical zoom of 2×. Images were obtained using a CCD camera (ORCA-ER).

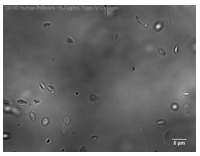

Video 3. **Increased TLR9 PLT surface expression results in type C CpG-mediated PLT clumping.** Washed human PLTs were transferred onto video chambers maintained at 37°C. Specific up-regulation of TLR9 surface expression in PLTs with 50 µg/ml type IV collagen preincubation had no effect on PLT morphology over a course of 20 min. Addition of 5 µM type C CpG to this PLT culture resulted in immediate PLT shape change and significant PLT clumping (characteristic of activation). Images were captured at 30-s intervals over the course of 72 min. Cells were viewed on an inverted microscope (TE-200) equipped with a 63× oil immersion objective, and images were obtained using a CCD camera (ORCA-ER). Time is indicated in minutes and seconds.

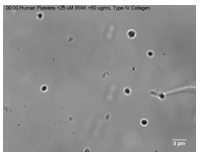

Video 4. **Increased TLR9 PLT surface expression results in type C CpG-mediated PLT clumping.** Washed human PLTs were transferred onto video chambers maintained at 37°C. Type C CpG-mediated PLT clumping was inhibited by preincubating PLTs with 20 µM IRAK-1/4 for 1 h before collagen IV incubation and type C CpG addition. Images were captured at 30-s intervals over the course of 72 min. Cells were viewed on an inverted microscope (TE-200) equipped with a 63× oil immersion objective, and images were obtained using a CCD camera (ORCA-ER). Time is indicated in minutes and seconds.

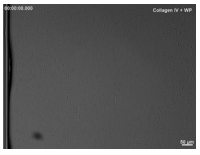

Video 5. **Vehicle control-treated washed PLTs do not form thrombi on collagen type IV.** Washed human whole-blood PLTs were pretreated with 5 µM vehicle control and perfused at a shear rate of 200 s^{-1} (flow rate of 18.7 µl/min) over a surface coated with type IV collagen for 10 min. Although addition of ODN to PLTs resulted in PLT clumping in the presence of type IV collagen, these did not form thrombi as compared with type I collagen (positive control). Addition of type C CpG did not result in increased thrombus formation relative to the ODN control in PRP on the type I collagen-coated surface. Cells were viewed on an inverted microscope (TE-200) equipped with a 63× oil immersion objective, and images were obtained using a CCD camera (ORCA-ER). Time is indicated in hours, minutes, and seconds. WP, washed PLTs. .

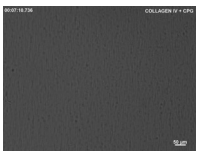

Video 6. **Type C CpG ODN-activated washed PLTs do not form thrombi on collagen type IV.** Washed human whole-blood PLTs were pretreated with 5 µM type C CpG ODN and perfused at a shear rate of 200 s^{-1} (flow rate of 18.7 µl/min) over a surface coated with type IV collagen for 10 min. Although addition of ODN to PLTs resulted in PLT clumping in the presence of type IV collagen, these did not form thrombi as compared with type I collagen (positive control). Addition of type C CpG did not result in increased thrombus formation relative to the ODN control in PRP on the type I collagen-coated surface. Cells were viewed on an inverted microscope (TE-200) equipped with a 63× oil immersion objective, and images were obtained using a CCD camera (ORCA-ER). Time is indicated in hours, minutes, and seconds.

Video 7. **Control ODN-activated washed PLTs do not form thrombi on collagen type IV.** Washed human whole-blood PLTs were pretreated with 5 µM control ODN and perfused at a shear rate of 200 s^{-1} (flow rate of 18.7 µl/min) over a surface coated with type IV collagen for 10 min. Although addition of ODN to PLTs resulted in PLT clumping in the presence of type IV collagen, these did not form thrombi as compared with type I collagen (positive control). Addition of type C CpG did not result in increased thrombus formation relative to the ODN control in PRP on the type I collagen-coated surface. Cells were viewed on an inverted microscope (TE-200) equipped with a 63× oil immersion objective, and images were obtained using a CCD camera (ORCA-ER). Time is indicated in hours, minutes, and seconds. WP, washed PLTs.

Video 8. **Type C CpG ODN-activated PRP PLTs do not form thrombi on collagen type IV.** Human PRP was pretreated with 5 µM type C CpG ODN and perfused at a shear rate of 200 s^{-1} (flow rate of 18.7 µl/min) over a surface coated with type IV collagen for 10 min. Although addition of ODN to PLTs resulted in PLT clumping in the presence of type IV collagen, these did not form thrombi, as compared with type I collagen (positive control). Addition of type C CpG did not result in increased thrombus formation relative to the ODN control in PRP on the type I collagen-coated surface. Cells were viewed on an inverted microscope (TE-200) equipped with a 63× oil immersion objective, and images were obtained using a CCD camera (ORCA-ER). Time is indicated in minutes and seconds.

Video 9. **Control ODN-activated PRP PLTs do not form thrombi on collagen type IV.** Human PRP was pretreated with 5 µM control ODN and perfused at a shear rate of 200 s^{-1} (flow rate of 18.7 µl/min) over a surface coated with type IV collagen for 10 min. Although addition of ODN to PLTs resulted in PLT clumping in the presence of type IV collagen, these did not form thrombi as compared with type I collagen (positive control). Addition of type C CpG did not result in increased thrombus formation relative to the ODN control in PRP on the type I collagen-coated surface. Cells were viewed on an inverted microscope (TE-200) equipped with a 63× oil immersion objective, and images were obtained using a CCD camera (ORCA-ER). Time is indicated in minutes and seconds.

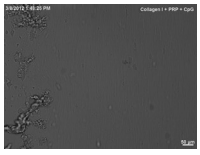

Video 10. **Type C CpG ODN-activated PRP PLTs form thrombi on collagen type I.** Human PRP was pretreated with 5 µM type C CpG ODN and perfused at a shear rate of 200 s^{-1} (flow rate of 18.7 µl/min) over a surface coated with type I collagen for 10 min. Although addition of ODN to PLTs resulted in PLT clumping in the presence of type IV collagen, these did not form thrombi as compared with type I collagen (positive control). Addition of type C CpG did not result in increased thrombus formation relative to the ODN control in PRP on the type I collagen-coated surface. Cells were viewed on an inverted microscope (TE-200) equipped with a 63× oil immersion objective, and images were obtained using a CCD camera (ORCA-ER). Time is indicated in hours, minutes, and seconds.

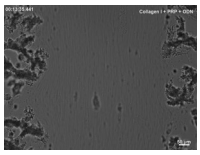

Video 11. **Control ODN-activated PRP PLTs form thrombi on collagen type I.** Human PRP was pretreated with 5 µM control ODN and perfused at a shear rate of 200 s^{-1} (flow rate of 18.7 µl/min) over a surface coated with type I collagen for 10 min. Although addition of ODN to PLTs resulted in PLT clumping in the presence of type IV collagen, these did not form thrombi as compared with type I collagen (positive control). Addition of type C CpG did not result in increased thrombus formation relative to the ODN control in PRP on the type I collagen-coated surface. Cells were viewed on an inverted microscope (TE-200) equipped with a 63× oil immersion objective, and images were obtained using a CCD camera (ORCA-ER). Time is indicated in hours, minutes, and seconds.